Hindawi
Mathematical Problems in Engineering
Volume 2019, Article ID 4264562, 16 pages
https://doi.org/10.1155/2019/4264562

Research Article

Mathematical Analysis of Optimal Operating Conditions in Heating Systems

Chan Kong, Yong Sun, Hongxi Zhang, and Yongjiang Shi

College of Energy and Environmental Engineering, Hebei Institute of Architecture and Civil Engineering, Zhangjiakou 075000, Hebei, China

Correspondence should be addressed to Yongjiang Shi; syj@hebiace.edu.cn

Received 7 January 2019; Accepted 31 March 2019; Published 6 May 2019

Academic Editor: Ali Ramazani

With changes in the outdoor air temperature, the heat consumption of buildings also changes. Timely adjustment of the heating systems to ensure optimal operating conditions is extremely significant to save energy. In this study, the operation conditions of a heating system were analyzed numerically, and the existence, uniqueness, and stability of the optimal operation conditions of the heating system were proved. An operation optimization model that could obtain the optimal operation conditions was also established, and the correctness of the model was verified experimentally. Experimental results showed that when the flow rate was 0.606 m^3/h, the supply water temperature was 67.13°C, water return temperature was 65.90°C, and the pump consumed the least amount of electricity. The experimental results and model calculation results showed that the operating cost is lower when the system flow rate is low and the supply water temperature is high under the same heat dissipation and indoor temperature.

1. Introduction

In the operation of heating systems, besides controlling and adjusting the operation parameters, it is necessary to adjust the heat supply according to the season, outdoor temperature, and heat demands of users [1]. The purpose is to make the heat dissipation from dissipating equipment adapt to the changing heat load, protect users from excessively high or low room temperatures, ensure that the user heat demand is met, and avoid unnecessary heat wastage to realize economic operation of heating systems [2].

Until now, several studies have been carried out on the optimized operation of heating systems, focusing on the establishment of mathematical models of water supply temperature, flow rate and outdoor temperature, and regulation of water supply temperature and flow rate. Atli Benonysson et al. [3] found that, in order to adapt to the change of heat load, frequent regulation of water supply temperature can reduce the operating costs, but they did not precisely state the frequency at which the water supply temperature was regulated. Guillaume Sandou and Sorin Olaru [4] applied the particle swarm optimization method to control district heating pipe networks and found that the optimization effect was different when the water supply temperature was adjusted at different frequencies. In addition, selection of the control cycle was an important part of the modeling problem [5]. Jonas Gustafsson et al. [6] controlled the radiator system and found that, compared with the traditional control, the larger temperature difference between the primary supply and return water could reduce the energy consumption of the pump and improve the overall fuel efficiency. Pengfei Jie et al. [7] established a dynamic model of the heating system network; based on this model, the peak valley method and correspondence analysis method were introduced, respectively, and two important parameters related to the dynamic characteristics of the heating system, i.e., delay time and relative attenuation degree, could also be calculated. It is concluded that the delay time is approximately equal to the time of heat media flow. These findings provide basis for the optimized operation and management of heating systems. Aibin Yan and Jun Zhao et al. [8] established the hydraulic model and found that, compared with the traditional central circulation pump, the distributed variable speed pump in the heating system could save at least 20% energy. In particular, when the distributed variable speed pump was used with low flow, more power could be saved. P. Lauenburg et al. [9]

developed a control algorithm for the radiator system based on field experiments and computer simulation. By determining the optimal combination of the water supply temperature and flow rate in the heating system, a low primary return water temperature was obtained, thereby reducing the operation costs. X. S. Jiang et al. [10] proposed an integrated regional direct heating energy system model that integrates wind energy, solar energy, natural gas, and electric energy. By establishing the objective function of the optimal control strategy with complex operation constraints, the fuel consumption was minimized and the operating efficiency of the system was improved. In other studies [11–13], the heat storage capacity of the district heating system was adapted to the large amounts of renewable energy conversion in the system, thus improving the system operation flexibility and economy. Based on outdoor temperature prediction and process data history, Laakkonen et al. [14] modeled delay as a distribution function and developed a robust optimizer to minimize pumping cost and heat loss; by optimizing the water supply temperature and flow rate, the heating system could run efficiently and smoothly. M. Leśko et al. [15] have presented different approaches to a simplified modeling of district heating networks for optimization purposes. Yiwen Jian et al. [16] analyzed an existing water temperature regulation mode and its impact on indoor environment and energy utilization on the basis of field investigation. By comparing the relationship among outdoor temperature, indoor temperature, indoor reference temperature, and water supply temperature, a method for optimizing water supply temperature based on simulation was proposed.

Hence, it can be seen that many researchers have worked in the field of optimized operation of heating system, but none have provided theoretical proofs regarding the properties of the optimal operating conditions of the heating system. Moreover, the optimal operation conditions will have different values under different constraints and objective functions.

Therefore, in this study, optimization of the operation of heating systems by adjusting the operating conditions according to load changes was performed, and the optimal operating conditions that can minimize the operating costs of the heating system were determined.

To improve the operating efficiency and reduce the operating costs of the heating system, mathematical analysis of the operating conditions was carried out. First, the existence, uniqueness, and stability of the operating conditions were proved. Then, an operation optimization model, with the lowest operating costs as the objective function and constraints imposed on the operating parameters to determine the optimal operating condition, was developed. Finally, the correctness of the model was verified experimentally. It is very important to regulate the heating system to determine whether the optimal operating condition is existent, unique, and stable. Through theoretical analysis and practical inspection, it was established that the method proposed in this paper improved the operation of the heating system.

The purpose of determining the optimal operating condition of the heating system is to minimize the operating costs while meeting the heating demands of users without considering the heat loss of the system. Regulating the heating system in time to ensure optimal operating conditions can not only save energy and costs, but also guide relevant research on the operating conditions. The optimal operating condition of the heating system discussed in this paper corresponds to a variable flow rate heating system.

2. Basic Concepts and Related Properties

2.1. Heat Supply and Heat Demand. The heating system considered in this study has n users and J heat sources as the research objects, and the collection of all users is represented as $N = \{1, \ldots, n\}$. The number of heat sources is J, denoted by the numbers $1, \cdots, J$. The relationship between the heat energy produced by heat source j and its users is represented as $\boldsymbol{y}_j = (y_{j1}, \cdots, y_{jn})$, where y_{ji} indicates that heat is supplied to user i within time τ. The heat energy production space of heat source j is $Y_j \subseteq R^J$, and the heat energy production set of all the heat sources is denoted as Y. The heat energy production set is a closed set, which satisfies convexity and strict convexity [17].

If the heat loss of the system is not considered, then the heat supplied to user i by the heat source is equal to the heat dissipated by user i.

Heat supplied by heat source j is

$$y_j = c\left(t_{gj} - t_{hj}\right) \cdot g_j \cdot \tau, \tag{1}$$

where t_{gj} is the water supply temperature of heat source j (°C), t_{hj} is the water return temperature of heat source j (°C), and g_j is the circulating flow rate of heat source j (kg/h).

The ratio of the heat obtained by user i from heat source j to the total heat produced by heat source j is $\theta_{ij} \in R^+$, $i = 1, 2, \cdots, n$. The heat that user i gets is

$$Q_i = \sum_{j=1}^{J} y_j \cdot \theta_{ij} = c \cdot \left(t_{gi} - t_{hi}\right) \cdot g_i \cdot \tau, \tag{2}$$

where t_{gi} is the supply water temperature for user i (°C), t_{hi} is the return water temperature for user i (°C), and g_i is the circulating flow rate of user i (kg/h).

The heat demand quantity x_i of user i should satisfy the condition $x_i \leq Q_i$; the heat constraint set is denoted as $B_i(g) = \{x_i \in X_i : x_i \leq Q_i\}$.

The heat demanded by user i at outdoor temperature t_w is

$$x_i = c\left(t_{gi}' - t_{hi}'\right) \cdot g_i \cdot \tau, \tag{3}$$

where c is the mass specific heat capacity of water (c=4187 J/(kg·°C)), t_{gi}' is the water supply temperature required by user i at outdoor temperature t_w (°C), t_{hi}' is the water return temperature of the heating user i at outdoor temperature t_w (°C), and g_i is the circulating flow rate required by heating user i at outdoor temperature t_w (kg/h).

2.2. Partially Optimal Relation in Heating Systems. Under the same heating quality, the heating system generates different operating costs in different operating conditions. Therefore,

choosing the optimal operating condition is extremely significant to reduce the operating costs of the system. The operating conditions of the heating system are reflected by the operating parameters, of which the main parameters are the flow rate and temperature. The two-dimensional vector (G, t) consisting of two parameters, flow rate and temperature, is called the operating parameter vector. The operating conditions under different operating parameter vectors will bring different operating results. The operating condition with better operating results is called the partially optimal condition, and based on the comparability of operating costs, the partially optimal relationship between operating parameter vectors is established [18].

2.3. Unit Mass Fluid Supply-and-Demand Heat Difference Function and Its Properties

2.3.1. Unit Mass Fluid Supply-and-Demand Heat Difference Function. (1) Total heat demand function of users is

$$\widehat{x}(\boldsymbol{g}) \cdot \boldsymbol{g} \cdot \tau = \sum_{i=1}^{n} x_i(g) = \sum_{i=1}^{n} c\left(t_{gi}{}' - t_{hi}{}'\right) \cdot \boldsymbol{g} \cdot \tau \quad (4)$$

$\widehat{x}(\boldsymbol{g}) = \sum_{i=1}^{n} c(t_{gi}{}' - t_{hi}{}')$, which is the required heat per unit mass of fluid at the outdoor temperature t_w. The flow rate vector $\boldsymbol{g} = (g_1, g_2, \cdots, g_n)$.

(2) Total heat supply function of heat sources is

$$\widehat{y}(\boldsymbol{g}) \cdot \boldsymbol{g} \cdot \tau = \sum_{j=1}^{J} y_j(g) = \sum_{i=1}^{n} c\left(t_{gi} - t_{hi}\right) \cdot g \cdot \tau \quad (5)$$

that is, $\widehat{y}(\boldsymbol{g}) = \sum_{i=1}^{n} c(t_{gi} - t_{hi})$, which is the heat per unit mass of fluid that the heat source supplies to users.

(3) The total heat demand and total heat supply difference function is

$$\begin{aligned}\widehat{z}(\boldsymbol{g}) \cdot \boldsymbol{g} \cdot \tau &= \widehat{x}(\boldsymbol{g}) \cdot \boldsymbol{g} \cdot \tau - \widehat{y}(\boldsymbol{g}) \cdot \boldsymbol{g} \cdot \tau \\ &= \sum_{i=1}^{n} c\left(t_{gi}{}' - t_{hi}{}'\right) \cdot \boldsymbol{g} \cdot \tau - \sum_{i=1}^{n} c\left(t_{gi} - t_{hi}\right) \\ &\quad \cdot \boldsymbol{g} \cdot \tau \\ &= \left(\sum_{i=1}^{n} c\left(t_{gi}{}' - t_{hi}{}'\right) - \sum_{i=1}^{n} c\left(t_{gi} - t_{hi}\right)\right) \cdot \boldsymbol{g} \\ &\quad \cdot \tau.\end{aligned} \quad (6)$$

Therefore, there is a unit mass fluid supply-and-demand heat difference function:

$$\widehat{z}(\boldsymbol{g}) = \sum_{i=1}^{n} c\left(t_{gi}{}' - t_{hi}{}'\right) - \sum_{i=1}^{n} c\left(t_{gi} - t_{hi}\right). \quad (7)$$

If $\widehat{z}(\boldsymbol{g}) > 0$, this means that the heat supply per unit mass of fluid is insufficient in the heating system; if $\widehat{z}(\boldsymbol{g}) < 0$, this means that there is a surplus heat supply per unit mass of fluid in the heating system; if $\widehat{z}(\boldsymbol{g})$=0, this means that the heating system provides enough heat per unit mass of fluid without wastage.

2.3.2. Properties of the Unit Mass Fluid Supply-and-Demand Heat Difference Function

(i) Supply-and-Demand Heat Difference Function Relation. In the process of heating, the heat demand of users should not be greater than the heat supply of heat sources [19]. That is,

$$\sum_{i=1}^{n} c\left(t_{gi}{}' - t_{hi}{}'\right) \cdot \boldsymbol{g} \cdot \tau \leqq \sum_{i=1}^{n} c\left(t_{gi} - t_{hi}\right) \cdot \boldsymbol{g} \cdot \tau. \quad (8)$$

(1) Strong supply-and-demand heat difference function relation is

$$\widehat{z}(\boldsymbol{g}) \cdot \boldsymbol{g} \cdot \tau = 0, \quad \forall \boldsymbol{g} \in {R_+}^N; \quad (9)$$

(2) weak supply-and-demand heat difference function relation is

$$\widehat{z}(\boldsymbol{g}) \cdot \boldsymbol{g} \cdot \tau \leqq 0, \quad \forall \boldsymbol{g} \in {R_+}^N. \quad (10)$$

(ii) Zero-Order Homogeneity. The second important property of the unit mass fluid supply-and-demand heat difference function $\widehat{z}(\boldsymbol{g})$ is zero-order homogeneity with respect to the flow rate vector $\boldsymbol{g}$; i.e., for any $\lambda > 0$, $\widehat{z}(\lambda \boldsymbol{g}) = \widehat{z}(\boldsymbol{g})$.

When it is proved that the optimal operation condition exists, to use Brouwer's fixed point theorem [20], the flow rate vector must be standardized in the following way:

$$g_i{}' = \frac{g_i}{\sum_{i=1}^{n} g_i}. \quad (11)$$

(iii) Single-Value Continuity. The unit mass fluid supply-and-demand heat difference function is $\widehat{z}(\boldsymbol{g}) = \sum_{i=1}^{n} c(t_{gi}{}' - t_{hi}{}') - \sum_{i=1}^{n} c(t_{gi} - t_{hi})$; therefore, to prove that it is a single-valued continuous function, it is necessary to prove that $\widehat{x}(\boldsymbol{g}) = \sum_{i=1}^{n} c(t_{gi}{}' - t_{hi}{}')$ and $\widehat{y}(\boldsymbol{g}) = \sum_{i=1}^{n} c(t_{gi} - t_{hi})$ are single-valued continuous functions [21].

(1) Proving that $\widehat{x}(\boldsymbol{g}) = \sum_{i=1}^{n} c(t_{gi}{}' - t_{hi}{}')$ is a single-valued continuous function.

Proof. First, it is essential to prove that for all $\boldsymbol{g} > 0$, the correspondence B_i defined by the heat constraint set $B_i(\boldsymbol{g}) = \{x_i \in X_i : x_i \leq Q_i\} = \{x_i \in X_i : x_i \leq \sum_{j=1}^{J} y_j(g) \cdot (1 - \varepsilon)\}$ is a continuous correspondence of a nonnull compact value [22]. Considering $\boldsymbol{g} > 0$, the heat constraint correspondence B_i is obviously nonnull compact, and it is subsequently proved that for $\boldsymbol{g} > 0$, it is a continuous correspondence.

Obviously, B_i is the upper semicontinuous correspondence, so it is only necessary to prove that it is also the lower semicontinuous correspondence [23].

Let $\boldsymbol{g} \in {R_+}^N$, $x_i \in B_i(\boldsymbol{g})$, and $\{\boldsymbol{g}_t\}$ be any sequence making $\boldsymbol{g}_t \longrightarrow \boldsymbol{g}$.

Let $I_i^t = \sum_{j=1}^{J} \boldsymbol{y}_j(\boldsymbol{g}_t) \cdot (1 - \varepsilon)$. As $\boldsymbol{y}_j(\boldsymbol{g}_t)$ is a heat energy production vector when the operating cost is the lowest and is continuous, $\boldsymbol{y}_j(\boldsymbol{g}_t) \geqq 0$, and I_i^t is continuous with respect

to $\boldsymbol{g}_t$. Thus, $I_i^t > 0$. Let us consider the following two cases:

Case 1 ($x_i < \sum_{j=1}^{J} y_j(g) \cdot (1-\varepsilon)$). Then, for any sequence $\{x_i^t\}$ that makes $x_i^t \longrightarrow x_i$, because of the continuity of I_i^t, when t is greater than some sufficiently large integer t', we have

$$x_i < I_i^t = \sum_{j=1}^{J} y_j\left(g_t\right) \cdot (1-\varepsilon). \tag{12}$$

Thus, $x_i^t \in B_i(\boldsymbol{g}_t)$.

Case 2 ($x_i = \sum_{j=1}^{J} y_j(g) \cdot (1-\varepsilon)$). Let $x_i^t = (I_i^t / x_i^t) x_i^t$. As $I_i^t / x_i^t \longrightarrow I_i / x_i = 1$, $x_i^t \longrightarrow x_i$. At the same time, for all t, $x_i^t = (I_i^t / x_i^t) x_i^t = I_i^t$, and thus $x_i^t \in B_i(\boldsymbol{g}_t)$. In this way, for all $\boldsymbol{g} > 0$, since B_i is the upper semicontinuous correspondence and lower semicontinuous correspondence, it is a continuous correspondence.

As the partially superior ordering $\succcurlyeq$ is continuous, the heat constraint set correspondence $\boldsymbol{B}_i$ is a continuous correspondence of nonnull compact values. According to the Berge maximum theorem [24], $x_i(\boldsymbol{g})$ is upper semicontinuous. According to the strict convexity of the partially superior ordering, $x_i(\boldsymbol{g})$ is a single-valued map. As the upper semicontinuous correspondence of the single-valued mapping is continuous, $x_i(\boldsymbol{g})$ is a single-valued continuous function. Thus, $\hat{x}(\boldsymbol{g})$ is a single-valued continuous function. □

(2) Proving that $\hat{y}(\boldsymbol{g}) = \sum_{i=1}^{n} c(t_{gi} - t_{hi})$ is a single-valued continuous function.

Proof. From the property of the production set, it can be seen that the production set is a bounded closed set (also known as a compact set) and satisfies strict convexity. According to the Walker maximum theorem [25], as $\forall \boldsymbol{g} \in {R_+}^N$, Y_j is compact, and $0 \in Y_j$, it is clear that $\boldsymbol{y}_j(\boldsymbol{g})$ is a nonnull upper semicontinuous correspondence.

Next, we prove that $\boldsymbol{y}_j(\boldsymbol{g})$ is a single-valued function. If $\boldsymbol{y}_j(\boldsymbol{g})$ is not a single-valued function, let ${\boldsymbol{y}_j}^1$ and ${\boldsymbol{y}_j}^2$ be two heat energy production vectors that ensure the least operating costs when, $\forall \boldsymbol{g} \in {R_+}^N$, ${\boldsymbol{y}_j}^1 \cdot \boldsymbol{g} \cdot \tau = {\boldsymbol{y}_j}^2 \cdot \boldsymbol{g} \cdot \tau$. According to the strict convexity of Y, $\lambda {\boldsymbol{y}_j}^1 + (1-\lambda){\boldsymbol{y}_j}^2 \in \operatorname{int} Y_j$, $\forall 0 < \lambda < 1$. Therefore, $t < 1$, which makes $t[\lambda {\boldsymbol{y}_j}^1 + (1-\lambda){\boldsymbol{y}_j}^2] \in \operatorname{int} Y_j$ true.

Thus, $t[\lambda {\boldsymbol{y}_j}^1 + (1-\lambda){\boldsymbol{y}_j}^2] = t\boldsymbol{g}{\boldsymbol{y}_j}^1 < \boldsymbol{g}{\boldsymbol{y}_j}^1$, which contradicts the assumption that ${\boldsymbol{y}_j}^1$ is a heat energy production vector that ensures the least operating costs. Thus, $\boldsymbol{y}_j(\boldsymbol{g})$ is a single-valued function. As the upper semicontinuous correspondence of the single-valued function is continuous, $\boldsymbol{y}_j(\boldsymbol{g})$ is a continuous single-valued function. Thus, $\hat{\boldsymbol{y}}(\boldsymbol{g})$ is a single-valued continuous function. □

(3) Proving that $\hat{z}(\boldsymbol{g}) = \sum_{i=1}^{n} c({t_{gi}}' - {t_{hi}}') - \sum_{i=1}^{n} c(t_{gi} - t_{hi})$ is a single-valued continuous function.

Proof. As $\hat{x}(\boldsymbol{g})$ and $\hat{y}(\boldsymbol{g})$ are single-valued continuous functions,

$$\begin{aligned} \hat{z}(\boldsymbol{g}) &= \sum_{i=1}^{n} c\left({t_{gi}}' - {t_{hi}}'\right) - \sum_{i=1}^{n} c\left(t_{gi} - t_{hi}\right) \\ &= \hat{x}(\boldsymbol{g}) - \hat{y}(\boldsymbol{g}); \end{aligned} \tag{13}$$

therefore, $\hat{z}(\boldsymbol{g})$ is also a single-valued continuous function. □

3. Proofs for Properties of the Optimal Operating Condition of the Heating System

3.1. Existence of the Optimal Operating Condition of the Heating System. The circulating flow rate in the heating system needs to consider the minimum inaccessible flow rate; therefore, the circulating flow rate cannot be infinitely small. Further, considering the properties of the pipeline medium, the water supply temperature cannot be infinitely large; that is, there is an upper limit value. The optimal operating condition is the combination of the circulating flow rate and water supply temperature, and the optimal operating flow rate and optimal water supply temperature are in a one-to-one correspondence relation, and they influence each other; hence, as long as there is evidence of the existence of an optimal operating flow rate, this means that there is an optimal operating condition.

For maintaining generality, the flow rate is limited to the following simplex [26] to examine the existence of the optimal operating condition [27–29]:

$$S = \left\{ \boldsymbol{g} \in {R_+}^N : \sum_{i=1}^{n} g^i = 1 \right\}. \tag{14}$$

In this study, the operating conditions of the heating system have partially superior orderings. For the heating system, $\hat{z}(\boldsymbol{g}) : S \longrightarrow R^N$ is a zero-order homogeneous continuous function, and it satisfies the weak supply-and-demand heat difference function relation; therefore, it can be proved that the optimal operating condition exists; i.e., $\boldsymbol{g}^* \in {R_+}^N$ making $\hat{z}(\boldsymbol{g}^*) \leqq 0$.

Proof. First, a continuous correspondence is constructed from a compact convex set [23] to itself. Then according to Brouwer's fixed point theorem, relevant conclusions are obtained.

The function f is defined as follows from the compact convex set S to itself: $S \longrightarrow S$:

$$f^i(\boldsymbol{g}) = \frac{g^i + \max\left\{0, \hat{z}^i(\boldsymbol{g})\right\}}{1 + \sum_{k=1}^{n} \max\left\{0, \hat{z}^k(\boldsymbol{g})\right\}}, \quad i = 1, 2, \cdots, n. \tag{15}$$

Note that if $f(x)$ and $h(x)$ are continuous, then $\max\{f(x), h(x)\}$ is continuous. Thus, the function f defined above is continuous.

As f is continuous and S is a compact convex set, according to Brouwer's fixed point theorem, there is a flow rate vector $\boldsymbol{g}^*$ such that $f(\boldsymbol{g}^*) = \boldsymbol{g}^*$.

$$g^{*i} = \frac{g^{*i} + \max\left\{0, \widehat{z}^i\left(\boldsymbol{g}^*\right)\right\}}{1 + \sum_{k=1}^{n} \max\left\{0, \widehat{z}^k\left(\boldsymbol{g}^*\right)\right\}}, \quad i = 1, 2, \cdots, n. \tag{16}$$

The following proves that the fixed point g^* is the optimal operating flow rate vector to be proved.

Multiplying $1 + \sum_{k=1}^{n} \max\{0, \widehat{z}^k(\boldsymbol{g}^*)\}$ on both sides of (36), we obtain $g^{*i} \sum_{k=1}^{n} \max\{0, \widehat{z}^k(\boldsymbol{g}^*)\} = \max\{0, \widehat{z}^i(\boldsymbol{g}^*)\}$.

Multiplying $\widehat{z}^i(\boldsymbol{g}^*)$ on both ends of the above equation and summing over i give

$$\begin{aligned} &\left[\sum_{i=1}^{n} g^{*i} z^i\left(\boldsymbol{g}^*\right)\right]\left[\sum_{i=1}^{n} \max\left\{0, \widehat{z}^i\left(\boldsymbol{g}^*\right)\right\}\right] \\ &= \left[\sum_{i=1}^{n} \widehat{z}^i\left(\boldsymbol{g}^*\right) \max\left\{0, \widehat{z}^i\left(\boldsymbol{g}^*\right)\right\}\right]. \end{aligned} \tag{17}$$

From the weak supply-and-demand heat difference function relation, we have $\sum_{i=1}^{n} g^{*i} \widehat{z}^i(\boldsymbol{g}^*) \leqq 0$ and $\sum_{i=1}^{n} \max\{0, \widehat{z}^i(\boldsymbol{g}^*)\} \geqq 0$; therefore, it can be inferred that

$$\sum_{i=1}^{n} \widehat{z}^i\left(\boldsymbol{g}^*\right) \max\left\{0, \widehat{z}^i\left(\boldsymbol{g}^*\right)\right\} \leqq 0. \tag{18}$$

As each item in the above summation is either 0 or $(\widehat{z}^i(\boldsymbol{g}^*))^2 \geqq 0$, to ensure that the above summation is less than or equal to 0, each item must be 0; namely, $\widehat{z}^i(\boldsymbol{g}^*) \leqq 0$, $i = 1, \cdots, n$. □

3.2. Uniqueness of Optimal Operating Condition of the Heating System. The above proofs demonstrate the existence of an optimal operating condition by analyzing the partially superior relation and supply-and-demand heat difference functions in the heating system. It is essential to prove that the optimal operating condition is unique. The so-called uniqueness means that there are no two or more linearly independent optimal operating flow rate vectors; otherwise, owing to the zero-order homogeneity, there will be an infinite number of proportional flow rates that are the optimal operating flow rate vectors.

Uniqueness Proof I. We assume that the flow rate vector is greater than 0. If $\boldsymbol{g}^*$ is the optimal operating flow rate of the heating system and the strong supply-and-demand heat difference function relationship is established, it can be proved that the optimal operating flow rate is unique.

Proof. With the flow rate vector being greater than 0, $\boldsymbol{g}^* > 0$. Let $\boldsymbol{g}$ be another optimal operating flow rate that is not proportional to $\boldsymbol{g}^*$. Suppose, for a certain user k, there is $m = \max_i(g^i/g^{*i}) = g^k/g^{*k}$.

According to the definitions of zero-order homogeneity and the optimal operating condition, $\widehat{z}(\boldsymbol{g}^*) = \widehat{z}(m\boldsymbol{g}^*) = 0$. As $m = g^h/g^{*h} \geqq g^i/g^{*i}, \forall i = 1, \cdots, n$, and h is such that $m > g^h/g^{*h}$, $mg^{*i} \geqq g^i, \forall i$ and $mg^{*h} > g^h$, when the flow rate for user k does not change and that for user h decreases relatively, the demand of user h remains unchanged; however, the supply becomes less, which makes $\widehat{z}^h(\boldsymbol{g}) > 0$, and obviously $\widehat{z}^h(\boldsymbol{g}) > 0$ contradicts $\widehat{z}(\boldsymbol{g}^*) = 0$. □

Uniqueness Proof II. We now consider another proof of the uniqueness of the optimal operating condition in the case where the supply-and-demand heat difference function satisfies the weak axiom of revealed partial optimization. The supply-and-demand difference function shows that the weak axiom of revealed partial optimization is defined as follows:

If $\boldsymbol{g}\widehat{z}(\boldsymbol{g}) \geqq \boldsymbol{g}\widehat{z}(\boldsymbol{g}')$, then $\boldsymbol{g}'\widehat{z}(\boldsymbol{g}) > \boldsymbol{g}'\widehat{z}(\boldsymbol{g}')$, $\forall \boldsymbol{g}, \boldsymbol{g}' \in R_+^N$. At this time, the supply-and-demand heat difference function is said to satisfy the weak axiom of revealed partial optimization [30].

The weak axiom of revealed partial optimization implies that the supply-and-demand heat difference function of the heating system under the flow rate vector $\boldsymbol{g}$ has $\widehat{z}(\boldsymbol{g})$ and $\widehat{z}(\boldsymbol{g}')$; however, $\widehat{z}(\boldsymbol{g})$ is the optimal supply-and-demand heat difference function for the flow rate vector $\boldsymbol{g}$; if it is unique, then $\widehat{z}(\boldsymbol{g}) \succ \widehat{z}(\boldsymbol{g}')$; therefore, $0 \geqq \widehat{z}(\boldsymbol{g}) > \widehat{z}(\boldsymbol{g}')$, so under the flow rate vector $\boldsymbol{g}'$, we have $\boldsymbol{g}'\widehat{z}(\boldsymbol{g}) > \boldsymbol{g}'\widehat{z}(\boldsymbol{g}')$.

If the strong supply-and-demand heat difference function relation and weak axiom of revealed partial optimization are established, then, for any $\boldsymbol{g} \neq k\boldsymbol{g}^*$, $\boldsymbol{g}^*\widehat{z}(\boldsymbol{g}^*) > 0$, and the optimal operating condition is unique, where $\boldsymbol{g}^*$ is the optimal operating flow rate.

Proof. We assume that $\boldsymbol{g}^*$ is the optimal operating flow rate, making $\widehat{z}(\boldsymbol{g}^*) \leqq 0$. According to the strong supply-and-demand difference function relation, $\boldsymbol{g}\widehat{z}(\boldsymbol{g}) = 0$, and thus $\boldsymbol{g}\widehat{z}(\boldsymbol{g}) \geqq \boldsymbol{g}\widehat{z}(\boldsymbol{g}^*)$. Thus, according to the weak axiom of revealed partial optimization, we have $\boldsymbol{g}^*\widehat{z}(\boldsymbol{g}) > \boldsymbol{g}^*\widehat{z}(\boldsymbol{g}^*) = 0 \Longrightarrow \boldsymbol{g}^*\widehat{z}(\boldsymbol{g}) > 0, \forall \boldsymbol{g} \neq k\boldsymbol{g}^*$.

For any $\forall \boldsymbol{g} \neq k\boldsymbol{g}^*$, $\boldsymbol{g}^*\widehat{z}(\boldsymbol{g}) > 0$ means that there is at least i making $\widehat{z}^i > 0$. Therefore, the optimal operating condition must be unique. □

3.3. Stability of the Optimal Operating Condition of the Heating System. Owing to the influence of outdoor air temperature and other factors, the operating parameters in the heating system are always fluctuating. When these parameters fluctuate, whether the heating system can automatically return to the original state of the optimal operating condition, that is, whether the optimal operating condition is stable, is another factor to be considered.

Assuming that the strong supply-and-demand difference function relation is established, if $\widehat{z}(\boldsymbol{g})$ satisfies the weak axiom of revealed partial optimization, the operating flow rate of the heating system is globally stable.

Proof. From the uniqueness of the optimal operating condition, we can infer that the optimal operating flow rate is unique because $\widehat{z}(\boldsymbol{g})$ satisfies the weak axiom of revealed

partial optimization. The Lyapunov function [31] is now defined as follows:

$$V(\boldsymbol{g}) = \sum_{i=1}^{n} \left(g^i(t) - g^{*i}\right)^2 = (\boldsymbol{g} - \boldsymbol{g}^*) \cdot (\boldsymbol{g} - \boldsymbol{g}^*). \quad (19)$$

According to the hypothesis of the weak axiom of revealed partial optimization, the optimal operating flow rate $\boldsymbol{g}^*$ is unique. In addition, as

$$\begin{aligned} \frac{dV}{dt} &= 2\sum_{i=1}^{n} \left(g^i(t) - g^{*t}\right) \frac{dg^i(t)}{dt} \\ &= 2\sum_{i=1}^{n} \left(g^i(t) - g^{*t}\right) \widehat{z}^i(\boldsymbol{g}) \\ &= 2\left[\boldsymbol{g}\widehat{z}(\boldsymbol{g}) - \boldsymbol{g}^*\widehat{z}(\boldsymbol{g})\right], \end{aligned} \quad (20)$$

from the strong supply-and-demand heat difference function relation, $\boldsymbol{g}\widehat{z}(\boldsymbol{g}) = 0$, so $dV/dt = -2\boldsymbol{g}^*\widehat{z}(\boldsymbol{g})$. From the uniqueness proof, we can see that $\boldsymbol{g}^*\widehat{z}(\boldsymbol{g}^*) > 0$ holds, so $dV/dt = -2\boldsymbol{g}^*\widehat{z}(\boldsymbol{g}) < 0$. Finally, the Lyapunov theorem [32] shows that $\dot{\boldsymbol{g}} = \widehat{z}(\boldsymbol{g})$ is globally stable with respect to $\boldsymbol{g} \neq k\boldsymbol{g}^*$. □

4. Establishment of the Operation Optimization Model

4.1. Objective Function. During the operation of the heating system, the operating costs of the heating unit mainly include the fuel costs for heating the heating medium, electricity costs resulting from the pumps driving the circulation of heat in the pipe network, electricity costs for the water replenishing pump, costs associated with the heat loss of the system, annual average costs of the project investment apportioned to the service life of the heat supply network, and costs pertaining to production organization and personnel. Among them, the latter four costs are not affected by changes in the independent variables or the effect is very small, so they are treated as constants. Therefore, when considering the operation costs of the system, the fuel costs and electricity costs associated with the circulating pumps driving the circulation of heat in the pipe network are mainly considered.

(1) Operating Costs Model of Unit Flow Rate Change. Now, we only regulate the circulating flow rate of the heating system without changing the water supply temperature. If the circulating flow rate of the system is increased, only the electricity costs associated with the circulating water pump are increased and not the operating costs under the operating condition before adjustment.

The circulating water pump is a mechanical device that drives the hot water circulating in the heating system. The formula [33] for calculating the shaft power of the circulating water pump is

$$N = \frac{G \times \Delta P \times 1000}{3600 \times \eta}, \quad (21)$$

where N is the shaft power of the circulating water pump (kW), G is the circulating flow rate of water (m^3/h), ΔP is the pressure difference between the outlet and inlet sections of the pump (MPa), and η is the total efficiency of the circulating water pump.

If the circulating flow rate of the system is increased, the power of the circulating water pump needs to be increased, which increases the electricity consumption. Obviously, the volume adjustment only changes the flow-head characteristic curve of the water pump without changing the pipe-network characteristic curve of the system.

When the flow rate increases 1 m^3/h, the extra power consumed by the pump is

$$N = \frac{(G+1) \times \Delta P \times 1000}{3600 \times \eta} - \frac{G \times \Delta P \times 1000}{3600 \times \eta}. \quad (22)$$

If the electricity price is j_d \$/kWh, the increased electricity cost is

$$\begin{aligned} K_1 &= j_d \cdot N \cdot \tau \\ &= j_d \times \left(\frac{(G+1) \times \Delta P \times 1000}{3600 \times \eta} - \frac{G \times \Delta P \times 1000}{3600 \times \eta}\right) \\ &\quad \times \tau, \end{aligned} \quad (23)$$

where τ is the operating time after system adjustment (h).

(2) Operating Costs Model of Unit Temperature Change. Now, we only regulate the water supply temperature without changing the circulating flow rate in the system. If the water supply temperature rises, only the fuel costs are increased and not the operating costs before adjustment.

When the water temperature increases by 1°C, the heat generated will increase in time τ.

$$Q = cm\Delta t = 4.187 \times 10^6 \times G \times \tau \times 1, \quad (24)$$

where c is the mass specific heat capacity of water (c=4187 J/(kg·°C)), m is the circulation flow rate of the system (kg(m=10^3×G·τ)), Δt is the temperature difference between the supply and return water (°C) of the system, and τ is the operating time after quality regulation (h).

The increased heat supply is provided by the combustion of the fuel, and the amount of heat generated after combustion of the additionally consumed fuel is equal to the increased heat supply, which is converted into standard coal (standard coal is a measure of energy, that is, 29,307 kJ (7,000 kilocalories) per kilogram of standard coal), giving

$$4.187G\tau = eN, \quad (25)$$

where e is the calorific value of standard coal (e = 29.307×10^3 MJ/t) and N is the amount of coal consumed (t).

The cost of the standard coal consumed is

$$K_2 = j_m \cdot N = 1.42866892 \times 10^{-4} G \cdot j_m \cdot \tau, \quad (26)$$

where K_2 is the total cost of the coal consumed (\$) and j_m is the price of standard coal (\$/t).

In summary, the operating costs are as follows:

$$K\left(\vec{F}\right) = \frac{G \times \Delta P \times 1000}{3600 \times \eta} \times j_d \tau + 1.42866892 \times 10^{-4} G\left(t_g - t_h\right) j_m \tau \quad (27)$$

where G is circulating flow rate in the system (t/h), j_d is the price of electricity (\$/kWh), j_m is the price of standard coal(\$/t), and τ is the number of operating hours after system adjustment.

Minimum operating costs are as follows.

$$K\left(\vec{F}\right) = \frac{G \times \Delta P \times 1000}{3600 \times \eta} \times j_d \tau + 1.42866892 \times 10^{-4} G\left(t_g - t_h\right) j_m \tau \quad (28)$$

4.2. Establishment of the Constraint Conditions. This study is mostly confined to the operation of the heating system from the viewpoints of the water supply temperature, temperature difference between water supply and return, system flow rate, and so on, obtaining a nonlinear optimization model with inequality constraints.

4.2.1. Constraint Condition for the Water Supply Temperature

$$t_{\min} \le t_g \le t_{\max}, \quad (29)$$

where $t_{\min}$ is the lower limit of the water supply temperature (°C), t_g is the water supply temperature (°C), and $t_{\max}$ is the upper limit of the water supply temperature (°C).

4.2.2. Constraint Condition for Temperature Difference between Supply and Return Water

$$\Delta t_{\min} \le t_g - t_h \le \Delta t_{\max}, \quad (30)$$

where $\Delta t_{\min}$ is the lower limit of the temperature difference between water supply and return (°C), t_h is the return water temperature (°C), and $\Delta t_{\max}$ is the upper limit of the temperature difference between water supply and return (°C).

4.2.3. Constraint Condition for Flow Velocity

$$C_{\min} \le C \le C_{\max}, \quad (31)$$

where $C_{\min}$ is the minimum allowable velocity in the pipe network (m/s) and $C_{\max}$ is the maximum allowable velocity in the pipe network (m/s).

4.2.4. Constraint Condition for Flow Rate. The flow rate in the pipe network is influenced by the driving power of the pump and should not be less than the minimum allowable flow rate of the pump [34] and should not be greater than the rated flow rate of the pump:

$$G_{\min} \le G \le G_{\max}, \quad (32)$$

where $G_{\min}$ is the minimum allowable flow rate of the pump (m^3/h) and $G_{\max}$ is the rated flow rate of the pump (m^3/h).

According to the literature [34], the minimum allowable flow rate of the pump in this paper is 20% of the rated flow rate.

4.2.5. Heat Dissipation Equals Heat Demand. If the heat loss of the system is not considered, then the actual heat dissipated by the dissipation equipment equals the heat consumption of the building; i.e.,

$$KF_s\left(t_{pj} - t_n\right) = q_v V\left(t_n - t_w\right), \quad (33)$$

where K is the coefficient of heat transfer of the heat dissipation equipment (W/(m^2/°C)), F_s is heat dissipation area of the heat dissipation equipment (m^2), t_{pj} is the average temperature of the heating medium in the heat dissipation equipment (°C), t_n is the design indoor temperature (°C), q_v is the heating volume heat index of the building (W/(m^3/°C)), V is the outer volume of the building (m^3), and t_w is the outdoor temperature(°C).

4.2.6. Heat Supply is Greater than or Equal to Heat Demand. The premise of the optimal operating condition is to meet the heat demand. Therefore, the actual heat supplied when the heating system is running should be greater than or equal to the heat consumption of the building. When the cost of operation is the minimum, the two quantities should be equal [35]; i.e.,

$$\frac{Gc\left(t_g - t_h\right)}{3600} = 1163G\left(t_g - t_h\right) = q_v V\left(t_n - t_w\right), \quad (34)$$

where G is the circulating flow rate of the system (m^3/h) and c is the mass specific heat capacity of water (c=4187 J/(kg·°C)).

4.2.7. Heat Dissipation is Equal to Heat Supply. The actual heat dissipated by the dissipation equipment is equal to the actual heat supplied when the heating system is running.

$$KF_s\left(t_{pj} - t_n\right) = \frac{Gc\left(t_g - t_h\right)}{3600} = 1163G\left(t_g - t_h\right) \quad (35)$$

In summary, when the outdoor temperature is t_w, the following optimization model is obtained.

$$\begin{aligned} \min \quad & K\left(\vec{F}\right) \\ & = \frac{G \times \Delta P \times 1000}{3600 \times \eta} \times j_d \tau + 1.428669 \\ & \quad \times 10^{-4} G\left(t_g - t_h\right) j_m \tau \\ \text{s.t.} \quad & t_{\min} \le t_g \le t_{\max} \\ & \Delta t_{\min} \le t_g - t_h \le \Delta t_{\max} \end{aligned}$$

$$
\begin{aligned}
&C_{\min} \le C \le C_{\max} \\
&G_{\min} \le G \le G_{\max} \\
&KF_s\left(t_{pj} - t_n\right) = q_v V\left(t_n - t_w\right) \\
&\frac{Gc\left(t_g - t_h\right)}{3600} = 1163G\left(t_g - t_h\right) \\
&= q_v V\left(t_n - t_w\right) \\
&KF_d\left(t_{pj} - t_n\right) = \frac{Gc\left(t_g - t_h\right)}{3600} \\
&= 1163G\left(t_g - t_h\right)
\end{aligned} \tag{36}
$$

5. Experiments

The operation optimization model presented in this paper is composed of the objective function and constraints. Taking the flow rate and water supply temperature as the influencing variables and the lowest operating cost as the objective function, the water supply temperature, the range of the temperature difference between the supply and return water, range of the flow velocity, and range of the flow rate are constrained according to the system operation and safety requirements without considering the heat loss of the system. In this case, the heat dissipation, heat supply, and heat demand are equal, and the optimal operating condition of the heating system is obtained. Further, it is essential to determine whether the optimal operating condition of the heating system meets the uniqueness and stability requirements.

The actual heating system has heat loss. An experimental platform was built to achieve the following objectives: obtaining the relationship for the pressure difference between the inlet and outlet of the pump and the flow rate, verifying the correctness of the operation optimization model, and judging whether the optimal operating condition of the heating system meets the uniqueness and stability criteria.

5.1. Experimental Design

5.1.1. Experimental System. In this experiment, we tested the data pertaining to the flow rate, water supply temperature of the radiator, water return temperature of the radiator, power consumption of the pump, inlet and outlet pressures of the pump, and so on. We also changed the flow rate of the system under the condition of an unchanged pipe-network characteristic curve; therefore, we had to change the pump frequency. In summary, the components of the experimental platform are the following: heat source, circulating water pump, heat dissipation equipment, flowmeter, frequency converter, electric energy meter, thermometer, and manometer. Except for the high water tank and its inner electric heating tubes and temperature sensor that were installed on the second floor, the other equipment and pipes were on the first floor. The flow chart of the experimental system is shown in Figure 1.

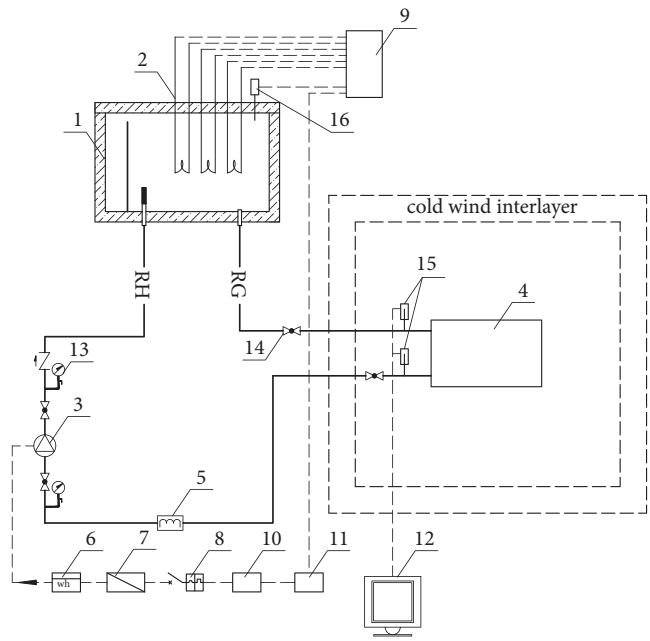

Figure 1: Flow chart of experimental system.

In Figure 1, the "RG" represents the water supply pipe, and "RH" represents the water return pipe.

The other components in the experimental system are labeled as follows: 1, high water tank; 2, electric heating tubes; 3, circulating water pump; 4, radiator; 5, electromagnetic flow meter; 6, electric energy meter; 7, inverter; 8, air switch; 9, control cabinet 1; 10, control cabinet 2; 11, total power supply; 12, computer; 13, pressure gauge; 14, ball valve; 15, temperature sensor 1; 16, temperature sensor 2.

The details are as follows:

A high water tank equipped with electric heating tubes was used to heat a room measuring 6 m × 6 m × 2.8 m, and the radiating equipment is a group of radiators; the return water of the system was pumped to the high water tank through a circulating water pump. An electromagnetic flow meter was installed at the inlet of the pump to measure the flow rate of the system; the inlet and outlet of the pump were equipped with pressure gauges.

To make the radiator dissipate heat steadily, a 12-cm-thick cold air interlayer was placed around the outside of the room, which is of the same height as the room. The fan was operated to supply air to the cold air interlayer through the air duct. The refrigerator was opened to refrigerate the air in the duct. The fan was controlled by control cabinet 2, and the refrigerator was controlled by control cabinet 1.

To ensure that the measured water supply and return temperature are closer to the radiator inlet and outlet water temperatures, we not only used insulation between the high water tank and radiator but also installed temperature sensor 1 on the inlet and outlet pipes of the radiator. The temperature of the supply and return water in this system was measured by temperature sensor 1 on the inlet and outlet pipes of the radiator. The room was equipped with indoor temperature measuring points; the high water tank was equipped with

Figure 2: Radiator and indoor measuring points.

temperature sensor 2, and the electric heating tubes in the high water tank were controlled by control cabinet 1. The indoor temperature and the inlet and outlet temperatures of the radiator displayed were on the computer; the temperatures of the high water tank and that of the cold air interlayer were displayed on the display screen in control cabinet 1; the converter frequency, flow rate of the system, inlet and outlet pressures of the pump, and power consumption of the pump were directly obtained from the corresponding equipment. The radiator and indoor measuring points are shown in Figure 2.

The circulating water pump was controlled by control cabinet 2, and its speed was controlled by the frequency converter. At the same time, an electric energy meter was installed between the circulating water pump and the frequency converter to measure the power consumption of the circulating water pump for a certain period.

5.1.2. Specifications of Laboratory Equipment. See Table 1 for details.

5.1.3. Test Conditions. Taking into account the system safety, experimental conditions, device parameters, and precision, the experiment was carried out using parameters in Table 2.

5.2. Experimental Principles. (1) The supply water temperature in the radiator, return water temperature in the radiator, and indoor temperature were measured, according to formula (37), to obtain the radiator heat sink [36].

$$Q = KF\left(\frac{t_g + t_h}{2} - t_n\right), \tag{37}$$

where Q is the heat dissipated in the radiator (W), K is the heat transfer coefficient of the radiator ($W/(m^2 \cdot {}^\circ C)$), F is the radiating area of the radiator (m^2), t_g is the inlet temperature of the radiator (°C), t_h is the outlet temperature of the radiator (°C), and t_n is the calculated temperature of the heating room (°C).

The heat dissipation per piece of the radiator used in this experiment satisfies formula (38).

$$Q = 0.533\left(\frac{t_g + t_h}{2} - t_n\right)^{1.313} \tag{38}$$

(2) In this experiment, the following parameters were not considered for validating the model as they did not influence the validity of the model: the supply and return water temperatures; the inlet and outlet water temperatures of the radiator; the heat loss between the high water tank and measuring point of the supply water temperature; and the return water temperature at the radiator.

5.3. Experimental Process. First, the heat load of the experimental room was set at 856.23 W. Next, without changing the settings of the system network, under the same heat dissipation and indoor temperature, by gradually increasing the frequency of the frequency converter to increase the flow rate of the pump, while adjusting the temperature of the high water tank and then changing the water supply temperature of the radiator, the abovementioned parameters were recorded. The recorded data are presented in Table 3.

5.4. Data Processing. Using the experimental data presented in Table 3, the heat dissipated from the radiator and the heat supplied by the system at the corresponding flow rates, supply water temperatures, and return water temperatures were obtained; these values are listed in Table 4.

Next, the correctness of the model was verified with and without considering the influence of pump efficiency on the operation costs of the heating system.

5.4.1. Experimental Results. According to (23), the electricity costs K_1 satisfies the following equation:

$$K_1 = j_d \cdot N \cdot \tau \tag{39}$$

where K_1 is the electricity costs (\$), j_d is the electricity price (\$/kWh, here j_d=0.086855\$/kWh), N is the shaft power of the circulating water pump (kW), and τ is the operating time after system adjustment (h, here τ = 1h).

Here $W = N \cdot \tau$ and W is the power consumption of the water pump within one hour, which is measured by the experiment.

According to (26), K_2, denoting the fuel costs, satisfies the following equation:

$$K_2 = j_m \cdot N = 1.42866892 \times 10^{-4} G \cdot j_m \cdot \tau \tag{40}$$

where K_2 is the fuel costs (\$), j_m is the price of standard coal (\$/t, here j_m=118.281\$/t), G is the circulating flow rate of water (m^3/h), and τ is the operating time after system adjustment (h, here τ = 1h).

The electricity costs and fuel costs can be calculated by substituting the experimental data into (23) and (26).

Using the results presented in Tables 3 and 4 and using equations (23) and (26), we obtained the electricity costs and fuel costs within an hour under the same radiator heat dissipation and indoor temperature. The sum of the two gives the operating costs under different operating conditions. The specific values are presented in Table 5.

The relationship among the flow rate, supply water temperature, and operating costs is shown in Figure 3.

As observed in Table 5, when the flow rate is 0.606 m^3/h, the supply water temperature is 67.13°C, the water

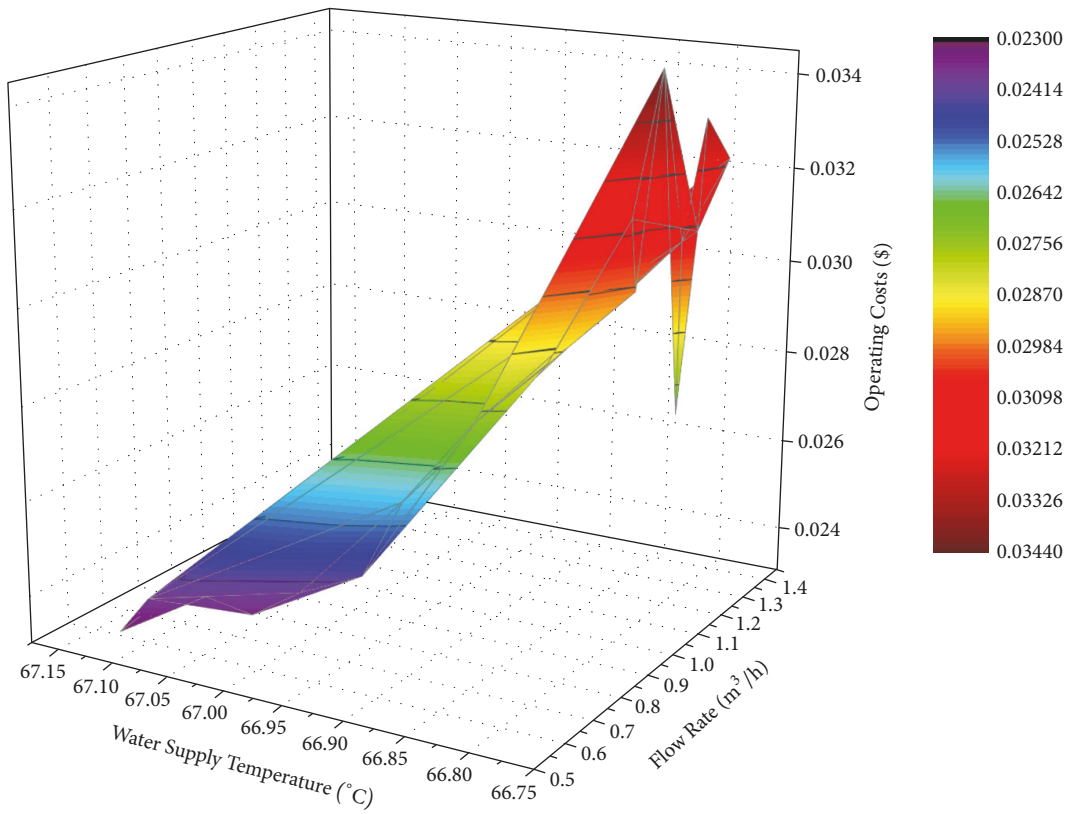

Figure 3: Relationship among flow rate, supply water temperature, and operating costs.

Table 1: Experimental equipment and its parameters.

Number	Equipment Name	Specifications and main parameters	Quantity	Remarks
1	Radiator	Cast-iron ellipsoidal four-column 760	10 pieces	
2	Electric heating tube	6kW	3	Resistance-type
3	High water tank	Length-0.75 m, width-0.45 m, and height-0.49 m	1	
4	Circulating water pump	Q=3.0m^3/h; H=35-12m; N=0.37kW	1	
5	Frequency converter	The power is 5.5 kW, the input voltage is was 380 V, and the output voltage is 0–380 V		
6	Pressure gauge	The measuring range is 0–0.6 MPa and the accuracy is 0.005 MPa		

return temperature is 65.90°C, and the pump consumes the least amount of electricity; the operation costs are the lowest, and there is only one operation condition with the lowest operation costs. Although the operating parameters changed during the experiment, they could always revert to the optimal operating condition, so the optimal operating condition of the heating system was stable.

5.4.2. Model Results. From Table 5, the relationship between the flow rate and power consumption at different pump frequencies could be obtained, as shown in Figure 4.

The relationship between flow rate and electric energy is as follows:

$$W = -0.448G^3 + 1.3152G^2 - 1.0977G + 0.405, \quad (41)$$

where G is the circulating flow rate of water (m^3/h).

Figure 4 showed that when the flow rate was 1.194 m^3/h, the power consumption fluctuates and when the flow rate was 1.276 m^3/h, it dropped to the lowest point. Now we discussed and analyzed them.

Firstly, when the flow rates were 1.194 m^3/h (29.50Hz) and 1.276 m^3/h (31.50Hz), we judge whether the points were operating in the high-efficiency zone of the pump. Multiple groups of flow rate and pressure difference data were measured at 29.50Hz and 31.50Hz, respectively, and Figures 5 and 6 were obtained, respectively. According to the experimental data, it was found that these two points were not in the high-efficiency zone of the pump.

The high-efficiency zone of the pump were located to the right of the hump peak of the pump characteristic curve, so

Table 2: Measuring parameter and its range.

Number	Measuring parameter	Testing range
1	Supply water	55–90°C
2	Temperature difference between supply and return water	0 ~15°C
3	Velocity	0.13–1.33 m/s
4	Flow rate	0.60–1.50 t/h

Table 3: Experimental data.

Number	Frequency	Flow Rate	Supply Water Temperature	Return Water Temperature	Indoor Temperature	Pump Inlet Pressure	Pump Outlet Pressure	Power Consumption
	Hz	m^3/h	°C	°C	°C	MPa	MPa	kWh
1	15.02	0.606	67.13	65.90	18.65	0.050	0.065	0.120
2	15.68	0.629	67.11	65.92	18.65	0.049	0.064	0.128
3	16.45	0.670	67.07	65.96	18.65	0.048	0.065	0.130
4	17.50	0.710	67.04	65.99	18.65	0.045	0.065	0.125
5	18.80	0.755	67.01	66.02	18.65	0.042	0.065	0.130
6	20.13	0.810	66.97	66.06	18.65	0.040	0.065	0.136
7	21.30	0.866	66.95	66.08	18.65	0.037	0.066	0.150
8	23.55	0.955	66.91	66.12	18.65	0.031	0.066	0.168
9	25.65	1.040	66.87	66.16	18.65	0.026	0.068	0.184
10	28.81	1.172	66.83	66.20	18.65	0.016	0.070	0.217
11	29.50	1.194	66.83	66.20	18.65	0.015	0.070	0.196
12	30.60	1.235	66.82	66.21	18.65	0.011	0.069	0.249
13	31.50	1.276	66.81	66.22	18.65	0.008	0.070	0.163
14	31.55	1.280	66.81	66.22	18.65	0.008	0.070	0.206
15	31.95	1.294	66.80	66.23	18.65	0.006	0.069	0.212
16	32.50	1.321	66.80	66.23	18.65	0.005	0.071	0.236
17	34.00	1.371	66.79	66.24	18.65	0.000	0.070	0.225

the points of 1.194 m^3/h (29.50Hz) and 1.276 m^3/h (31.50Hz) were not in the efficient zone of the pump.

Secondly, we judge whether the experimental data satisfied the relationship between frequency and flow rate, pressure difference, and power consumption.

The relationship between frequency of converter and system flow, pressure difference, and shaft power is

$$\frac{G_1}{G_2} = \frac{f_1}{f_2},$$
$$\frac{H_1}{H_2} = \frac{{f_1}^2}{{f_2}^2}, \quad (42)$$
$$\frac{N_1}{N_2} = \frac{{f_1}^3}{{f_2}^3}$$

where G_1, G_2 are the circulating flow rate of water (m^3/h); f_1, f_2 are the frequency of the converter (Hz); H_1, H_2 are the pressure difference (MPa); and N_1, N_2 are the power consumption (kWh).

Using the data of this experiment, we can obtain the relationship between frequency and flow rate, pressure difference, and power consumption and the relationship between flow rate and power consumption, which are represented in Figures 7, 8, 9, and 10, respectively.

It can be seen that the frequency of the converter and flow rate meet the relation $G_1/G_2 = f_1/f_2$; the frequency of the converter and pressure difference meet the relation $H_1/H_2 = {f_1}^2/{f_2}^2$; and the frequency of the converter and power consumption meet the relation

$$\frac{N_1}{N_2} = \frac{{f_1}^3}{{f_2}^3}. \quad (43)$$

Through the above analysis, we can find the fluctuating points were not in the high-efficiency zone of the pump, the experimental data also meet the relationship between frequency and flow rate, pressure difference, and power consumption, so the reason for this may be starting from 1.194 m^3/h (at this time, the frequency of the convert is 29.50 Hz), and the test data are beyond the frequency range of frequency converter, showing the gross error of inaccuracy.

Table 4: Heat dissipated and supplied under various flow rates and supply and return water temperatures.

Number	Flow Rate	Water Supply Temperature	Water Return Temperature	Indoor Temperature	Heat Dissipated	Heat Supplied
	m^3/h	˚C	˚C	˚C	W	W
1	0.606	67.13	65.90	18.65	856.23	866.98
2	0.629	67.11	65.92	18.65	856.23	870.62
3	0.670	67.07	65.96	18.65	856.23	865.03
4	0.710	67.04	65.99	18.65	856.23	867.13
5	0.755	67.01	66.02	18.65	856.23	869.40
6	0.810	66.97	66.06	18.65	856.23	857.37
7	0.866	66.95	66.08	18.65	856.23	876.35
8	0.955	66.91	66.12	18.65	856.23	877.56
9	1.040	66.87	66.16	18.65	856.23	858.90
10	1.172	66.83	66.20	18.65	856.23	858.86
11	1.194	66.83	66.20	18.65	856.23	874.99
12	1.235	66.82	66.21	18.65	856.23	876.31
13	1.276	66.81	66.22	18.65	856.23	875.72
14	1.280	66.81	66.22	18.65	856.23	878.46
15	1.294	66.80	66.23	18.65	856.23	857.97
16	1.321	66.80	66.23	18.65	856.23	875.87
17	1.371	66.79	66.24	18.65	856.23	877.13

Table 5: Electricity costs, fuel costs, and operation costs under different operating conditions.

Number	Flow Rate	Water Supply Temperature	Water Return Temperature	Indoor Temperature	Power Consumption	Electricity Costs	Fuel Costs	Operating Costs
	m^3/h	˚C	˚C	˚C	kWh	$	$	$
1	0.606	67.13	65.90	18.65	0.120	0.0104	0.0126	0.0230
2	0.629	67.11	65.92	18.65	0.128	0.0111	0.0126	0.0238
3	0.670	67.07	65.96	18.65	0.130	0.0113	0.0126	0.0239
4	0.710	67.04	65.99	18.65	0.125	0.0109	0.0126	0.0235
5	0.755	67.01	66.02	18.65	0.130	0.0113	0.0126	0.0239
6	0.810	66.97	66.06	18.65	0.136	0.0118	0.0125	0.0243
7	0.866	66.95	66.08	18.65	0.150	0.0130	0.0127	0.0258
8	0.955	66.91	66.12	18.65	0.168	0.0146	0.0128	0.0273
9	1.040	66.87	66.16	18.65	0.184	0.0160	0.0125	0.0284
10	1.172	66.83	66.20	18.65	0.217	0.0189	0.0125	0.0314
11	1.194	66.83	66.20	18.65	0.196	0.0170	0.0127	0.0297
12	1.235	66.82	66.21	18.65	0.249	0.0216	0.0127	0.0343
13	1.276	66.81	66.22	18.65	0.163	0.0141	0.0127	0.0269
14	1.280	66.81	66.22	18.65	0.206	0.0179	0.0128	0.0306
15	1.294	66.80	66.23	18.65	0.212	0.0184	0.0125	0.0309
16	1.321	66.80	66.23	18.65	0.236	0.0205	0.0127	0.0332
17	1.371	66.79	66.24	18.65	0.225	0.0195	0.0127	0.0323

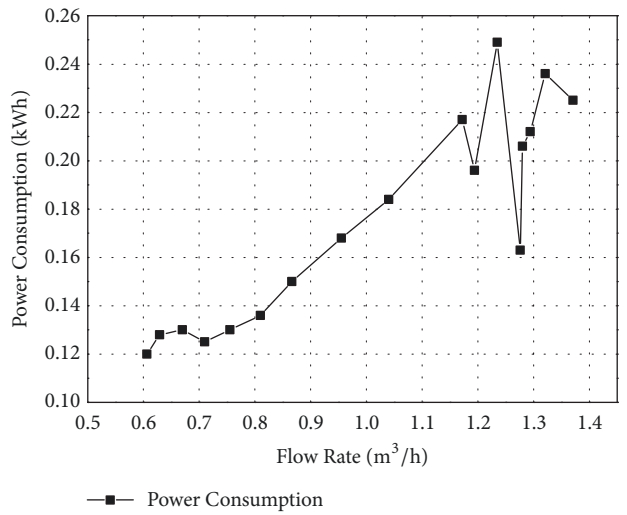

Figure 4: Relationship between flow rate and power consumption.

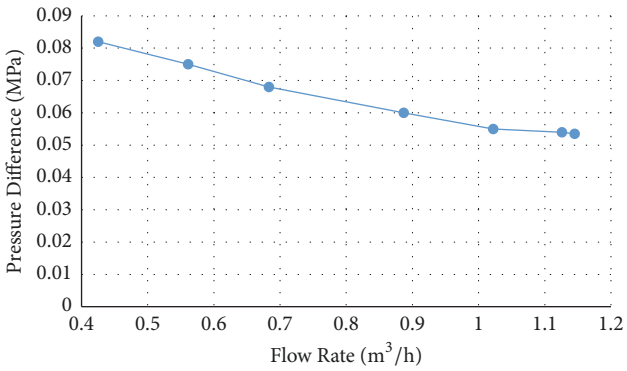

Figure 5: Relationship between the flow rate and the pressure difference in 29.50Hz.

When the flow rate was 1.276 m^3/h, the power consumption showed an obvious decline; on the one hand, it is because of the test error; on the other hand, it is because the point had exceeded the test range of frequency converter and was in a fluctuating state. Therefore, when the flow rate was 1.276 m^3/h, the power consumption decreased.

Finally, from Figure 10, it can be seen that when the flow rate was 1.194 m^3/h, the shaft power started to fluctuate, but the formula fitted by Figure 4 can still satisfy the relation between flow rate and shaft power before fluctuation, and in this paper, the optimal operating conditions obtained are not in the fluctuating part, so even if the above gross error occurred, it will not affect the conclusion of this paper.

Equation (41) is to substitute the basic parameters of the experiment into the objective function of the optimization model equation (36), so that the model results and the experimental results can be compared under the same basic parameters. Formula (41) is valid for the flow within the power consumption unfluctuating range.

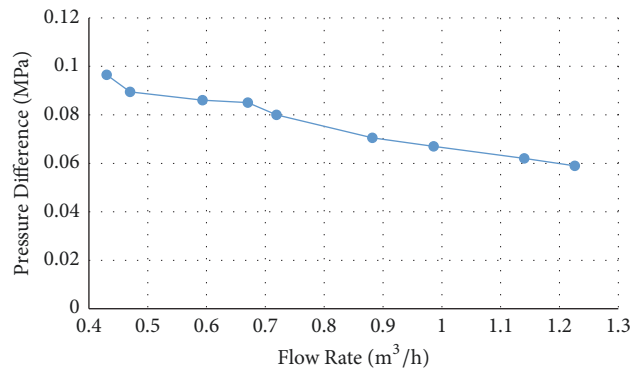

Figure 6: Relationship between the flow rate and the pressure difference in 31.50Hz.

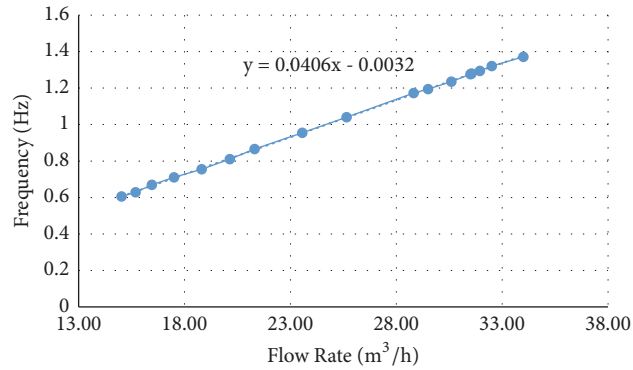

Figure 7: Relationship between flow rate and frequency.

Substitute (41) into the objective function of (36), the objective function of (36) becomes as follows.

$$\begin{aligned}\min \quad & K\left(\vec{F}\right) \\ &= \left(-0.448G^3 + 1.3152G^2 - 1.0977G + 0.405\right) \\ &\times 0.086855 + 1.42866892 \times 10^{-4} G \cdot \left(t_g - t_h\right) \\ &\times 118.281 \times 1\end{aligned} \tag{44}$$

In addition, the heat dissipated of each piece of radiator in this experiment meets the following equation:

$$\begin{aligned}Q &= KF\left(\frac{t_g + t_h}{2} - t_n\right) = KF\left(t_{pj} - t_n\right) \\ &= 0.533\left(\frac{t_g + t_h}{2} - t_n\right)^{1.313}\end{aligned} \tag{45}$$

where F is the radiating area per radiator (m^2).

The radiator used in this experiment is 10 pieces, so the heat dissipated of the radiator Q_s meets

$$Q_s = KF_s\left(t_{pj} - t_n\right) = 0.533\left(\frac{t_g + t_h}{2} - t_n\right)^{1.313} \times 10 \tag{46}$$

where F_s is the radiating area of 10 pieces of radiator (m^2) ($F_s = 10F$).

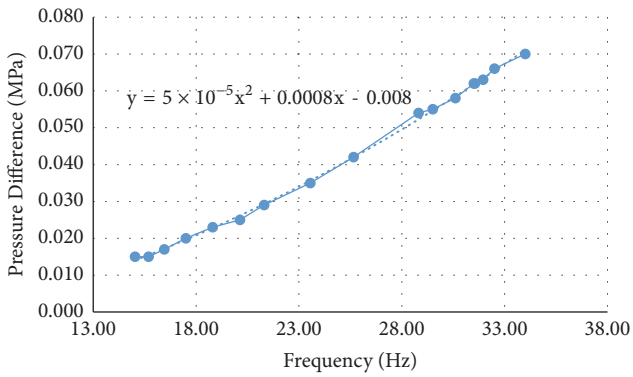

Figure 8: Relationship between frequency and pressure difference.

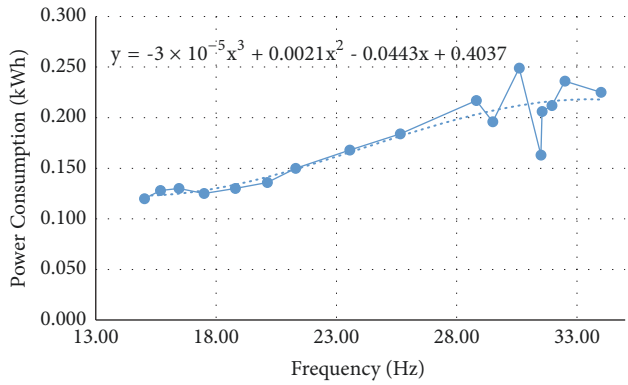

Figure 9: Relationship between frequency and power consumption.

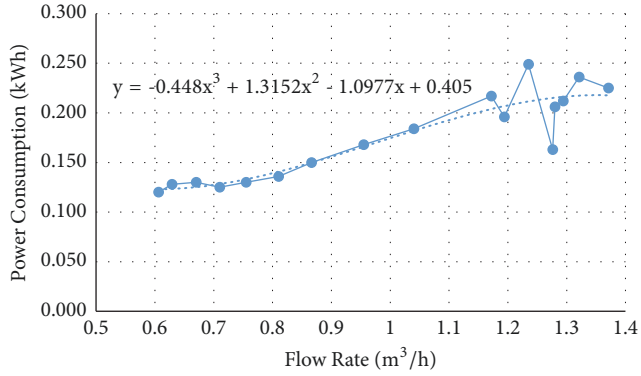

Figure 10: Relationship between flow rate and power consumption.

Furthermore, according to Section 5.1.3, this experiment is carried out under certain constraints of water supply temperature, temperature difference between supply and return water, flow velocity, and flow rate. The constraint condition and (46) are simultaneously substituted into the constraint conditions in (36), and we can obtain the following.

$$\begin{aligned} 55 \le t_g \le 90 \\ 0 < t_g - t_h \le 15 \\ 0.13 \le C \le 1.33 \\ 0.60 \le G \le 1.50 \\ 0.533\left(\frac{t_g + t_h}{2} - t_n\right)^{1.313} \times 10 = q_v V\left(t_n - t_w\right) \\ 1163G\left(t_g - t_h\right) = q_v V\left(t_n - t_w\right) \\ 0.533\left(\frac{t_g + t_h}{2} - t_n\right)^{1.313} \times 10 = 1163G\left(t_g - t_h\right) \end{aligned} \tag{47}$$

Finally, combined with (44) and (47), the operation optimization model of this experiment can be obtained as follows.

$$\begin{aligned} \min \quad & K\left(\vec{F}\right) = N \times 0.086855\tau + 1.42866892 \\ & \times 10^{-4} G\left(t_g - t_h\right) \times 118.281 \times 1 \\ & + 1.42866892 \times 10^{-4} \mathrm{G}\left(t_g - t_h\right) \times 118.281\tau \\ & = \left(-0.448G^3 + 1.3152G^2 - 1.0977G + 0.405\right) \\ & \times 0.086855 + 1.42866892 \times 10^{-4} G \cdot \left(t_g - t_h\right) \\ & \times 118.281 \times 1 \\ \text{s.t.} \quad & 55 \le t_g \le 90 \\ & 0 < t_g - t_h \le 15 \\ & 0.13 \le C \le 1.33 \\ & 0.60 \le G \le 1.50 \\ & 0.533\left(\frac{t_g + t_h}{2} - t_n\right)^{1.313} \times 10 = q_v V\left(t_n - t_w\right) \\ & 1163G\left(t_g - t_h\right) = q_v V\left(t_n - t_w\right) \\ & 0.533\left(\frac{t_g + t_h}{2} - t_n\right)^{1.313} \times 10 = 1163G\left(t_g - t_h\right) \end{aligned} \tag{48}$$

(49)

At the beginning of the experiment, the heat load of the room was 856.23 W. The numerical value was put into the operation optimization model and the following unique optimal solution was obtained.

$$\begin{aligned} \mathrm{K} &= 0.0231\$ \\ \mathrm{G} &= 0.6033\ \mathrm{m}^3/\mathrm{h} \\ \mathrm{t_g} &= 67.12514^{\circ}\mathrm{C} \\ \mathrm{t_h} &= 65.90478^{\circ}\mathrm{C} \end{aligned} \tag{50}$$

5.5. Discussion. In this experiment, the temperature sensors were set at the inlet and outlet of the radiator, so the

temperature values used for calculations were the inlet and outlet water temperatures of the radiator, without considering the heat loss between the high water tank and the inlet and outlet temperature measurement points of the radiator; the results pertaining to the operating costs were not affected. The heat load used in this experiment was 856.23 W, and the heat supply ranged from 857.37 to 878.46 W, with little heat loss.

The operating condition with the lowest operating cost determined experimentally is almost equal to the optimal operating condition determined using the model. The minimum operating cost obtained experimentally is 0.0001 $ less than that obtained using the model, which can be considered approximately equal. This error was caused by fitting the relationship between the flow rate and power, and the difference is within the allowable range of error. As the minimum operating costs obtained experimentally are almost equal to those determined using the model, the correctness of the model is established. It can be seen from the experimental results and model calculation results that the operating cost is lower when the system flow rate is low and the supply water temperature is high under the same heat dissipation and indoor temperature.

The experimental and model calculation results indicate that the operating condition with the minimum operating costs is unique; during the experiment, although the operating parameters were changing, they could always return to the optimal operating condition, so the optimal operating condition of the heating system can become stable.

First, this study developed a mathematical optimization model with the minimum operating cost as the objective function under the constraints of satisfying the heating demand and the safe and stable operation of the heating system. Second, with the same heat load, indoor temperature, and range of experimental parameters, the operating costs were determined and the operating condition with the minimum operating costs was identified. Furthermore, the nonlinear programming model having inequality constraints with the same heat load, indoor temperature, and parameter range as in the experiment was solved, and the optimal operating condition of the heating system was obtained; it can be judged that the optimal operating condition of the heating system is unique and stable. Finally, comparison between the experimental results and the model calculation results shows that with the same heat dissipation and the same indoor temperature, if the flow rate of the system is low and supply water temperature is high, the operating costs are lower, which proves the correctness and validity of the model.

6. Conclusion

First, an operation parameter vector composed of the flow rate and temperature of the heating system was mathematically defined. Second, a partial optimum relationship between the operation parameter vectors on the basis of comparable operation costs was established. Third, the optimal operation model with the lowest operating costs as the objective function and constraints on the operation parameter vector was established. Then the characteristics of the optimal operating conditions of the heating system were studied theoretically, and the existence, uniqueness, and stability of the optimal operating conditions of the heating system were proved. Finally, the correctness of the model was verified experimentally. It is proved that the operation optimization model developed in this study is reasonable and effective. Therefore, applying this model to optimize and adjust the heating system can lead to effective heating and economical operation of the heating system.

This model was only verified experimentally; the next step is to apply the operation optimization model to an actual heating system and ensure economical operations through optimal regulation of the heating system.

Data Availability

The data used to support the findings of this study are included within the article.

Conflicts of Interest

The authors declare that there are no conflicts of interest regarding the publication of this article.

Acknowledgments

The authors thank the Renewable Energy Heating Engineering Research Center for funding and the graduate innovation fund project of the Hebei Institute of Architecture and Civil Engineering (the project number is XA201720) for the support in performing the experiments. Further, the authors thank Shan Wan for the suggestions regarding the discussion on the partial optimization in this article.

References

[1] M. Wang and Q. Tian, "Dynamic heat supply prediction using support vector regression optimized by particle swarm optimization algorithm," *Mathematical Problems in Engineering*, vol. 2016, Article ID 3968324, 10 pages, 2016.

[2] Z. Shi, *Operation Regulation and Control of Heating System*, Tsinghua University Press, Beijing, China, 1994.

[3] A. Benonysson, B. Bøhm, and H. F. Ravn, "Operational optimization in a district heating system," *Energy Conversion and Management*, vol. 36, no. 5, pp. 297–314, 1995.

[4] G. Sandou and S. Olaru, "Particle swarm optimization based NMPC: an application to district heating networks," *Nonlinear Model Predictive Control*, vol. 384, pp. 551–559, 2009.

[5] K. C. B. Steer, A. Wirth, and S. K. Halgamuge, "Control period selection for improved operating performance in district heating networks," *Energy and Buildings*, vol. 43, no. 2-3, pp. 605–613, 2011.

[6] J. Gustafsson, J. Delsing, and J. van Deventer, "Experimental evaluation of radiator control based on primary supply temperature for district heating substations," *Applied Energy*, vol. 88, no. 12, pp. 4945–4951, 2011.

[7] P. Jie, Z. Tian, S. Yuan, and N. Zhu, "Modeling the dynamic characteristics of a district heating network," *Energy*, vol. 39, no. 1, pp. 126–134, 2012.

[8] A. Yan, J. Zhao, Q. An, Y. Zhao, H. Li, and Y. J. Huang, "Hydraulic performance of a new district heating systems with

distributed variable speed pumps," *Applied Energy*, vol. 112, no. 12, pp. 876–885, 2013.

[9] P. Lauenburg and J. Wollerstrand, "Adaptive control of radiator systems for a lowest possible district heating return temperature," *Energy and Buildings*, vol. 72, pp. 132–140, 2014.

[10] X. S. Jiang, Z. X. Jing, Y. Z. Li, Q. H. Wu, and W. H. Tang, "Modelling and operation optimization of an integrated energy based direct district water-heating system," *Energy*, vol. 64, pp. 375–388, 2014.

[11] Z. Gu, C. Kang, X. Chen, J. Bai, and L. Cheng, "Operation optimization of integrated power and heat energy systems and the benefit on wind power accommodation considering heating network constraints," *Proceedings of the Chinese Society of Electrical Engineering*, vol. 35, no. 14, pp. 3596–3604, 2015.

[12] X. Y. Chen, C. Q. Kang, M. O. Malley et al., "Increasing the flexibility of combined heat and power for wind power integration in China: modeling and implications," *IEEE Transactions on Power Systems*, vol. 30, no. 4, pp. 1848–1857, 2015.

[13] Z. Li, W. Wu, J. Wang, B. Zhang, and T. Zheng, "Transmission-constrained unit commitment considering combined electricity and district heating networks," *IEEE Transactions on Sustainable Energy*, vol. 7, no. 2, pp. 480–492, 2016.

[14] L. Laakkonen, T. Korpela, J. Kaivosoia et al., "Predictive supply temperature optimization of district heating networks using delay distributions," *Energy Procedia*, vol. 116, pp. 297–309, 2017.

[15] M. Lesko and W. Bujalski, "Modeling of district heating networks for the purpose of operational optimization with thermal energy storage," *Archives of Thermodynamics*, vol. 38, no. 4, pp. 139–163, 2017.

[16] Y. Jian, X. Liu, and Y. Li, "Simulation-based method for optimization of supply water temperature of room heating system," *Procedia Engineering*, vol. 205, pp. 3397–3404, 2017.

[17] A. Mas-Colell, M. D. Whinston, and J. Green, *Microeconomic Theory*, Oxford University Press, UK, 1995.

[18] S. Wan, *Establishment and Application of Partial Optimal Relation and Optimal Function of Heating System [M.S. thesis]*, Hebei University of Architecture, China, 2017.

[19] O. D. Hart, "On the optimality of equilibrium when the market structure is incomplete," *Journal of Economic Theory*, vol. 11, no. 3, pp. 418–443, 1975.

[20] D. Xia, S. Yan, W. Shu, and Y. Tong, *The Second Course of Functional Analysis*, Higher Education Press, Beijing, China, 2nd edition, 2008.

[21] H. Li, *Complex Variables Functions*, National Defence Industry Press, Beijing, China, 2011.

[22] Z. Wang, Z. Zuo, and Z. Li, *Economic Topology Method*, Peking University press, Beijing, China, 2002.

[23] G. Shoga, *Topology Tutorial—Topological Space and Distance Space, Numerical Functions, Topological Vector Space*, Higher Education Press, Beijing, China, 2nd edition, 2009.

[24] C. Berge, *Topological Spaces*, Dover Publications, New York, NY, USA, 2010.

[25] M. Walker, "A generalization of the maximum theorem," *International Economic Review*, vol. 20, no. 1, pp. 267–272, 1979.

[26] J. R. Mancles, *Algebraic Topological Basis*, Science press, Beijing, China, 2006.

[27] J. Geanakoplos, "An introduction to general equilibrium with incomplete asset markets," *Journal of Mathematical Economics*, vol. 19, no. 1-2, pp. 1–38, 1990.

[28] R. Radner, "Existence of equilibrium of plans, prices, and price expectations in a sequence of markets," *Econometrica*, vol. 40, no. 2, pp. 289–303, 1972.

[29] G. Tian, *Advanced Microeconomics*, vol. I, China Renmin University Press, Beijing, China, 2016.

[30] J. Han, *Terms of Trade and China's Economic Welfare*, China Economic Press, Beijing, China, 2016.

[31] X. Liao, *Theory Methods and Application of Stability*, Huazhong University of Science and Technology Press, Wu Han, China, 2nd edition, 2010.

[32] K. Duan, *Basic Theory of Stability and Lyapunov Function Construction*, Xinjiang University Press, Urumchi, China, 1990.

[33] Y. Lu, *Practical Handbook for Heating and Air Conditioning Design*, vol. 1, China Building Heating Press, China, 2008.

[34] Y. Zhang, "Centrifugal pump minimum flow to determine," *The International Journal of Fluid Machinery and Systems*, vol. 24, no. 1, pp. 44–47, 1996.

[35] P. Jie, N. Zhu, and D. Li, "Operation optimization of existing district heating systems," *Applied Thermal Engineering*, vol. 78, pp. 278–288, 2015.

[36] P. He, G. Sun, F. Wang, and H. Wu, *Heating Engineering*, China Building Heating Press, China, Fourth edition, 2009.